Effect of freeze–thaw cycles on load transfer between the biomineral and collagen phases in bovine dentin

A.C. Deymier-Black [a,*], J.D. Almer [b], D.R. Haeffner [b], D.C. Dunand [a]

[a] Department of Materials Science and Engineering, Northwestern University, Evanston, IL 60208, USA
[b] Advanced Photon Source, Argonne National Laboratory, Argonne, IL 60439, USA

ARTICLE INFO

ABSTRACT

Stabilization of biological materials by freezing is widespread in the fields of medicine and biomaterials research and yet, in the case of hard biomaterials such as dentin, there is not a good understanding of how such treatments might affect the mechanical properties. The freezing and thawing may have a number of different effects on dentin including formation of cracks in the microstructure and denaturation of the collagen. Using high-energy synchrotron X-ray diffraction, the apparent moduli of bovine dentin samples were measured before and after various numbers of freeze–thaw cycles. It was determined that repeated freezing and thawing has no measurable effect on the hydroxyapatite or fibrillar apparent moduli up to 10 cycles. This confirms that the use of low temperature storage for stabilization of dentin is reasonable in cases where stiffness is a property of importance.

© 2011 Elsevier B.V. All rights reserved.

1. Introduction

One of the key challenges in examining the mechanical properties of mineralized biomaterials, such as bone and dentin, is choosing an environment for storage and subsequent testing of harvested samples without demineralization of the ceramic phase, denaturation of the organic components, or dehydration of the specimen, all of which may affect the measurement. To limit these degrading effects, a number of techniques have been implemented including stabilization in phosphate buffered saline (PBS) solution and freezing.

Cryopreservation is used extensively in medicine for conservation of tissues and other biological materials [1]. In tissue banks, hard biological materials are usually maintained frozen for years in cryoprotectant solutions and at extremely low temperatures (−80 to −180 °C). Under these conditions, no changes in the strength or elastic modulus of human cortical bone [2] were measured after 5 years or in the permeability [3] and microleakage [4] of human permanent dentin after 3 months. Recently, however, there has been an increase in biomedical research which requires storage of biological tissues. In a research laboratory environment, it becomes more challenging to maintain biological samples at the extreme conditions used in tissue banks and instead samples are often stored in readily available commercial freezers (−10 to −25 °C). Studies have shown that long-term storage at these temperatures has no significant effect on the hardness of

permanent human dentin after 12 days [5], on the elastic modulus of human cortical bone after 1 month [6], or on the tensile modulus of permanent bovine dentin after 1 year [7].

More focus is however needed on the effect of repeated freezing and thawing of these hard biological tissues. During research investigations of dentin and bone, it is often necessary to repeatedly freeze and thaw samples for sample extraction, sample preparation, and sample testing. Cyclical freezing and thawing could have a number of effects on the properties of hard tissue such as dentin that contains a ceramic phase (hydroxyapatite, HAP), an organic phase (collagen and other proteins), and a liquid phase (water, saliva or PBS). Changes in the mechanical behavior could be caused by cracking associated with the volumetric expansion during freezing of water in biological structures such as dentinal tubules or the degradation of collagen. Using nano-indentation, Guidoni et al. found that although the modulus of human permanent dentin decreased by 20–28% after storage at −15 °C for an unknown period of time [8], contrary to the previously described studies [5–7], further freeze–thaw cycling had no significant effect. They theorize that the initial decrease in elastic modulus is due to cracking associated with ice formation in the tubules. The effect of freezing and freeze–thaw cycling on collagen is also unclear.

Much like the dentin studies, a number of collagen freezing studies have shown that some mechanical properties (e.g., elastic modulus and creep behavior) of rabbit ligaments [9] and human tendons [10] are not affected by freezing at −80 °C or cyclical freezing and thawing at −20 °C. However, some of these same studies observe a decrease in ultimate tensile strength (UTS) and a decrease in denaturation temperature [10]. These changes are further supported by reports of significant decreases in the UTS and Young's modulus of porcine [11]

* Corresponding author. Tel.: +1 847 491 5933; fax: +1 847 491 7820.
E-mail addresses: AlixDeymier2010@u.northwestern.edu (A.C. Deymier-Black), almer@aps.anl.gov (J.D. Almer), haeffner@aps.anl.gov (D.R. Haeffner), dunand@northwestern.edu (D.C. Dunand).

and human tendon [12] with freezing at −30 °C and freeze–thaw cycling at −20 °C. It is believed that these changes in collagen mechanical properties may be due to dehydration [12] or denaturation [10] of the collagen during freezing.

With both the microstructure of dentin and the molecular structure of collagen at possible risk during freeze–thaw cycling, it is important to examine its effects on dentin. The variability in the reported effects of freezing and freeze–thaw cycling on dentin and collagen mechanical properties makes it difficult to understand the effects of freezing on dentin structure. The conflicting results are likely due to errors associated with the measurement techniques and the spatial inhomogeneity of dentin. To better understand the effects of freeze–thaw cycling on both the ceramic and collagenous phases of dentin, the present study uses synchrotron X-ray diffraction to probe the effect of freeze–thaw cycles on the average load-bearing capacity of these two phases. Synchrotron X-ray diffraction has been previously performed on bone and teeth [13–19] subjected to load/unload cycles, but without emphasis on the previous sample freeze–thaw history which was assumed to be innocuous. In the present study, similar measurements of collagen and HAP average elastic strains during in situ compressive loading are performed, allowing determination of the load transfer between these two phases as a function of the number of freeze–thaw cycles. Any change in load transfer behavior may indicate internal damage such as cracks, degradation at the HAP/protein interface and change of protein stiffness due to degradation.

2. Methods

2.1. Sample preparation

The lower jaw of a healthy 18-month-old cow was acquired immediately following death (Aurora Packing Company, North Aurora, IL) and maintained at ambient temperature. One and a half hours after acquisition, six deciduous incisors (second, third and fourth incisors from both sides of the jaw) were extracted using dental tools. The teeth were then mechanically cleaned with a scalpel blade to remove excess tissue and pulp from the tooth surface and pulpal cavity, and placed in Dulbecco's PBS solution (Invitrogen, Carlsbad, CA) at ambient temperature. The incisors were mounted in a low speed diamond saw where parallel cuts were made perpendicular to the root's long axis below the cementum–enamel junction. These cuts were made 6–8 mm apart, depending on the incisor size. This resulted in twelve pure root dentin samples with a height of 5.5–7.5 mm, two parallel sides, and the natural tooth cross-section consisting of a hollow near cylinder. The teeth were maintained hydrated during preparation by dripping PBS solution during mounting and by using deionized water as a lubricant during cutting. After cutting, the samples were immediately re-immersed in ambient-temperature PBS solution.

2.2. Freeze–thaw cycles

The twelve samples were transported in ambient-temperature PBS to Argonne National Laboratory (ANL, Argonne, IL) where X-ray diffraction experiments were performed at the Advanced Photon Source (APS). The samples were randomly separated into four categories with three samples in each, labeled O, A, B and C. The O samples underwent diffraction measurements while they were fresh and were subsequently frozen. Samples in group A were tested in the fresh, uncycled condition, as well as after 5 freeze–thaw cycles. Diffraction measurements for the B samples were taken before cycling, after 5 freeze–thaw cycles, and after 10 freeze–thaw cycles. The control samples, C, were never frozen but measurements were taken at time intervals equivalent to the others. Therefore, all twelve samples (A, B, C, O) were measured before cycling, six samples (A, B) were measured after five freeze–thaw cycles, and three samples (B) were measured after ten freeze–thaw cycles.

The freezing was performed in a commercial freezer at a temperature of −25 °C. The samples, which remained immersed in approximately 1 ml of PBS solution at all times, were placed in the freezer for 80 min. The samples were then removed from the freezer and left to thaw at ambient temperature for 60 min. This was repeated for the appropriate number of cycles immediately followed by diffraction measurements.

2.3. Thermal history

To confirm that the tested dentin samples were fully frozen during the 80 min in the commercial freezer, the temperature of similar dentin samples was measured under identical conditions. Three dentin samples, which were extracted from a different animal but prepared according to the methods described above, were thawed and blotted dry to remove any excess PBS from the pulpal cavity. An unsheathed thermocouple was placed into the pulpal cavity so that its junction was approximately halfway between the top and bottom of the sample. The cavity was sealed on both ends using silicone putty creating a waterproof seal around the thermocouple. The thermocouple–dentin setup was immersed in 1 ml of Dulbecco's PBS solution in a small sealable tube identical to those used during freeze–thaw testing and placed in the same commercial freezer. Temperature measurements were recorded every 5 min for 80 min.

To better understand the behavior of Dulbecco's PBS solution, 1 ml of solution was placed in a small sealable tube and frozen for 80 min in the same commercial freezer. The sample was then left to thaw at ambient temperature (~20 °C). Since melting temperature and freezing temperature are expected to be equivalent, the recorded temperature at the point when the solution around the thermocouple junction became liquid was taken as the PBS freezing temperature.

2.4. Diffraction measurements

The high-energy X-ray diffraction measurements were performed at ambient temperature, approximately 27 °C, at beam-line 1-ID-C of the APS. A schematic of the experimental setup is shown in Fig. 1 and a detailed description is given in Ref. [15]. Uniaxial compressive loading of the dentin cylinders was carried out in increments of 10 MPa from 0 MPa to 50 MPa, well below the plastic region of dentin [20]. Wide angle X-ray (WAXS) and small-angle X-ray (SAXS) scattering measurements were taken at 8–10 locations, depending on the sample size, along a line in the buccal–lingual direction of the tooth (Fig. 2). The monochromatic 65 keV X-ray beam used for the diffraction measurements had a cross-sectional area of $30 \times 50 \ \mu m^2$ and was used in transmission, thus sampling a volume large enough to contain many dentinal tubules and both intertubular and peritubular dentins. This allowed for measurement of the average phase strains in dentin. The sampling locations were spaced 0.5 mm apart and located at the vertical center of the dentin samples, 2.75–3.75 mm from either platen depending on the sample height.

The WAXS diffraction rings arise from the crystalline HAP phase and were recorded using a MAR165 CCD (165 mm diameter, 80 μm pixels) placed at a sample-to-detector distance of 678 mm. The SAXS diffraction patterns were recorded using a Princeton Instruments CCD ($20 \times 22 \ mm^2$, 22.5 μm pixels) at a sample-to-detector distance of 4000 mm. The SAXS patterns display well-defined peaks (see Fig. 3) which arise from the ~67 nm periodic gap spacing of the collagen matrix. In the case of mineralized tissue, the primary SAXS contrast associated with these peaks is between the relatively dense HAP particles, which are formed within the gaps, and the collagen matrix. Changes in the measured SAXS spacing with applied load therefore represent changes in the average HAP particle spacing, which in turn results from cooperative deformation between the collagen and HAP particles. Thus, the SAXS-derived strain provides the composite response on the nanoscale level (without the effects from the larger
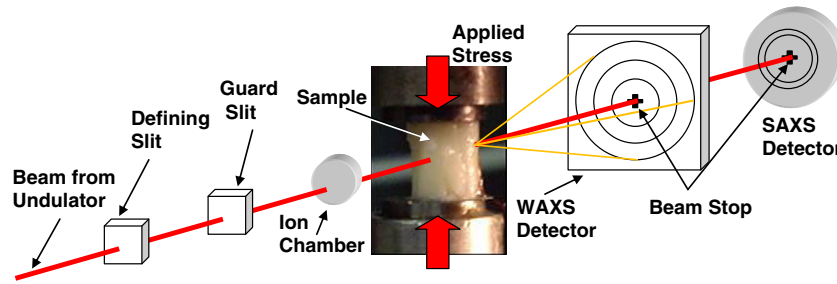
Fig. 1. Schematic of the experimental diffraction setup showing a photograph of the bovine dentin sample. The height of the sample is 7.5 mm.

microstructure such as the tubules), and will therefore be described as the fibrillar strain. A disk of pure pressed ceria powder (CeO₂, NIST Standard Reference Material SRM-674a) which was inserted at the beginning and end of the diffraction series was used as a standard. During the entire experimentation time, the samples were kept hydrated in a small bath of ambient temperature PBS solution using a custom hydration rig attached to the lower platen.

2.5. Diffraction analysis

Typical WAXS and SAXS diffraction patterns are shown in Fig. 3. To determine lattice spacing, procedures presented in Refs. [21–25] were followed and are summarized here. First, the calibration parameters including beam center, detector tilt, and sample-to-camera distance were determined using a number of ceria reflections. These parameters were then used to convert the diffraction patterns from polar (radius (pixels) vs. azimuth (degrees)) to Cartesian (x–y pixels) coordinates. The HAP (00.2), HAP (22.2), and HAP (00.4) peaks were fit to pseudo-Voigt functions as a function of radius and azimuth (η), yielding the peak position at each azimuth $R_{hkl}(\eta)$. The radial stress-free value for a given reflection, $R_{o,hkl}$, was determined as the intersection of $R_{hkl}(\eta)$ for a number of applied loads, as detailed in Refs. [13,22]. The internal lattice strain was then determined according to the equation $\varepsilon_{hkl}(\eta) = (R_{0,hkl} - R_{hkl}(\eta))/R_{hkl}(\eta)$. From plots of $\varepsilon_{hkl}(\eta)$ vs. η, the axial and transverse strain components for a given reflection, $e_{11} = \varepsilon(\eta = 90°, 270°)$ and $e_{22} = \varepsilon(\eta = 0°, 180°)$, respectively, were found using equations derived by He and Smith for two-dimensional detectors [26].

SAXS patterns were calibrated using Ag-behenate standard, and transformed using similar procedures as for the WAXS data. The radial peak center of the third order mineralized SAXS peak, $R(\eta)$ was measured and referenced to the radial peak center at which no stress was applied ($R^* = R(\eta)$ at $p = 0$). The associated fibrillar strain was determined in the longitudinal direction ($\eta = 90, 270 \pm 15°$), according to $e_{11} = (R^* - R(\eta))/R(\eta)$. It is notable that due to the absence of a strain-free standard (as opposed to the WAXS-determined strains), residual strains cannot be determined for the SAXS data.
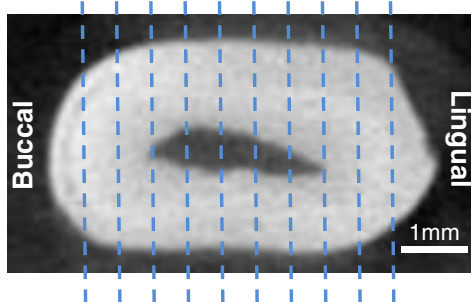
With known values of e_{11}^{HAP}, e_{22}^{HAP}, and e_{11}^{coll} from the diffraction patterns, it is possible to plot the phase strains as a function of applied stress. These plots are linear, and are thus uniquely defined by their slope, called the apparent modulus ($E_{app} = \sigma_{applied}/\varepsilon$) representing the in-situ elastic modulus of the phase in the presence of load transfer. For each sample, the apparent modulus values measured at the first and last points, those nearest the sample edges, were eliminated. This data was considered unreliable due to the oval sample shape, which leads to a small near-edge thickness and thus low diffraction intensity. The consequential low intensity makes fitting and analysis difficult and introduces large errors. As a result 6–8 apparent elastic modulus values were determined for each sample, depending on size. For each measurement of the apparent modulus, the sample received a total radiation dose of ~240 kGy. While such doses have been shown to impact fracture behavior, we expect little effect on the apparent moduli, as increases in collagen stiffness (i.e., due to cross-linking by radiation) are unlikely to affect load transfer significantly, given the much higher Young's modulus of HAP [27,28].

2.6. Micro-computed tomography

After diffraction measurements, the samples were maintained hydrated in PBS and frozen at −20 °C. The cross-sectional area of the samples was obtained through laboratory micro-computed tomography measurements using a Scanco Medical MicroCT 40 system (Scanco Medical, Southeastern, PA, USA). The samples were placed in a flat bottomed polymer cup filled with PBS solution. The microfocus X-ray tube was operated at 70 kV and 114 µA, and the beam passed through a 0.13 mm thick Be window on the X-ray tube and through a 0.50 mm thick Al filter before encountering the sample. With this cone beam system, 20 projections were collected over a 0.300 s integration time for each projection with a 1024 pixel diameter. Reconstruction using the instrument software was on a 1024×1024 grid with 30.7 µm voxels (volume elements).

The cross-sectional area of each specimen at the approximate position where the X-ray scattering measurements were collected was determined from reconstructed cross-sections, allowing an exact determination of the applied stress in the diffraction volume. In this determination, the standard threshold for bone histomorphometry suggested by the manufacturer, verified for bone of adults of various species in the scanner used in this study and confirmed for bovine dentin was used to differentiate the mineralized tissue from the other less absorbing material, such as the PBS and plastic container. Specifically, the threshold was 200 on a scale of 0 to 1000 corresponding to linear attenuation coefficients of 0 to 8 cm⁻¹, respectively.

2.7. Statistical analysis

Determination of significant differences between the means of residual strain and HAP and fibrillar apparent moduli for populations that were uncycled, cycled 5 times and cycled 10 times were
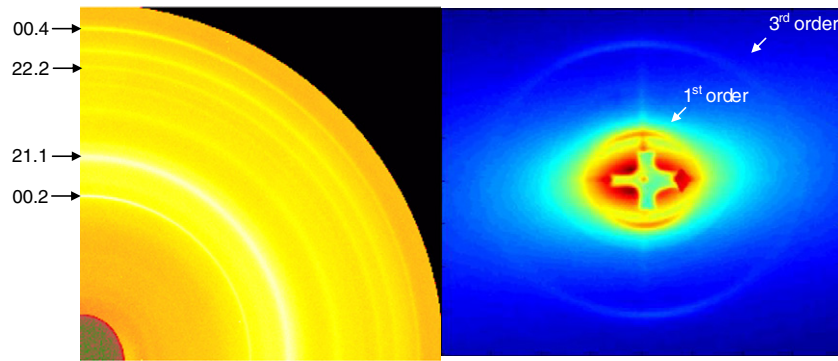

Fig. 2. Lab micro-computed tomography image of a sample from group O taken from the bottom of a left third incisor. The dotted lines represent the path of the beam during measurement.

Fig. 3. Example of WAXS and SAXS diffraction patterns.

measured by one-way ANOVA (analysis of variance) using Origin 7 (Origin Lab, Northampton, MA, USA). The same ANOVA tests were used to compare the mean HAP and fibrillar apparent moduli at different locations within dentin and between tooth types (2nd, 3rd, and 4th incisors). ANOVA tests were performed at a significance level of $p < 0.05$.

In the case where significant differences were measured, multiple t-tests were used to determine which of the population means differed. The significance level on the t-tests was also $p < 0.05$.

3. Results

The thawing temperature of the pure PBS solution was -1.3 ± 0.2 °C. The immersed dentin samples reached -1.3 °C within 10–20 min (Fig. 4) and the -25 °C freezer temperature after about 50 min, maintaining that temperature for at least 30 min.

Representative plots of HAP and fibrillar elastic strain vs. applied stress are shown in Fig. 5, from which the phase apparent elastic moduli are determined as best-fit slopes. Table 1 gives the average apparent HAP and fibrillar moduli for the various dentin sample populations, determined by averaging the apparent modulus values from the 6 to 8 points in each sample to obtain sample averages and then averaging these values from all samples in a given population. These average HAP and fibrillar apparent moduli are all within error of each other, independent of the number of freeze–thaw cycles. The
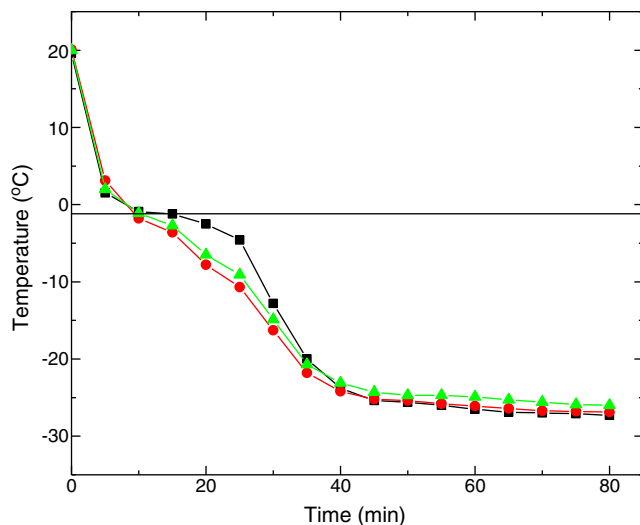
average apparent moduli measured from the control samples, C, are also constant within error, and equal to those of populations O, A, and B.

As described above, HAP and fibrillar apparent elastic modulus measurements were taken at six to eight locations across the width of every sample, as shown in Fig. 2, to account for intra-sample variations. The variation from point to point within a sample was quite large. The average standard deviations for each dentin sample among the twelve uncycled samples (C, O, A, B) were 5.9 and 4.1 GPa for HAP and the fibril respectively. The average intra-sample standard deviations for the six samples (A, B) with 5 freeze–thaw cycles were 6.4 GPa for HAP and 4.2 GPa for the fibril. Finally for the three samples subjected to 10 cycles (B), the average intra-sample standard deviations were 6.1 and 3.4 GPa, respectively. The mean values of both the HAP and the fibrillar moduli increased significantly from the buccal edge to the lingual edge of the samples. There was no significant difference between the mean HAP and fibrillar moduli measured for the 2nd, 3rd, or 4th bovine incisor.

When comparing the population means of the HAP apparent elastic modulus for the populations of samples that were uncycled (C, O, A, B), cycled 5 times (A, B), and cycled 10 times (B) no significant difference was measured ($p < 0.05$) as shown in Fig. 6. Also, when comparing the HAP apparent modulus population mean of each uncycled sample, after 5 freeze–thaw cycles, and after 10 freeze–thaw cycles, no significant differences could be found for any of the individual samples.
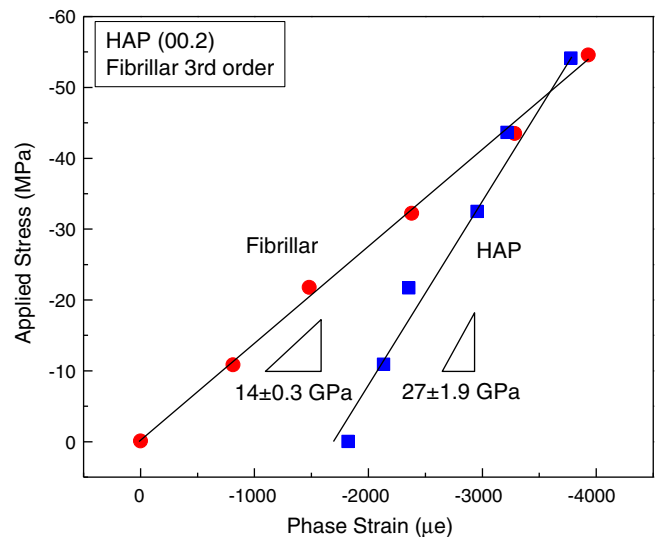

Fig. 4. Plots of internal temperature as a function of time for three dentin samples frozen in 1 ml of PBS solution at -25 °C for 80 min. The horizontal line represents the freezing temperature of the PBS solution.

Fig. 5. Plot of applied stress vs. longitudinal elastic strain for the fibril (SAXS) and HAP (WAXS, HAP (00.2) reflection) for a point located 2.5 mm from the buccal edge and 2 mm from the lingual edge in a fresh, uncycled dentin sample taken from the bottom of a fourth incisor on the right side of the jaw from the point of view of the animal.

Table 1
Apparent moduli of HAP and the fibril in dentin as a function of freeze–thaw cycles. Note that the variation in the average HAP and fibrillar moduli with freezing treatment is extremely small.

Number of freeze–thaw cycles	0	5	10
HAP			
E_{app}^{HAP} (GPa)	28 ± 4.1 (O, A, B)	28 ± 4.6 (A, B)	28 ± 3.2 (B)
$E_{app}^{HAP} control$ (GPa)	30 ± 2.5 (C)	29 ± 1.9 (C)	27 ± 2.8 (C)[a]
Fibril			
E_{app}^{fib} (GPa)	18 ± 2.3 (O, A, B)	18 ± 3.5 (A, B)	17 ± 3.5 (B)
$E_{app}^{fib} control$ (GPa)	19 ± 0.6 (C)	18 ± 0.4 (C)	17 ± 1.2 (C)[a]

[a] There is only one control sample measured at a time equivalent to 10 freeze–thaw cycles, for that reason, the error here represents the variation between the 8 points in the sample and not the variation between multiple samples in a population.

Similarly, as seen in Fig. 6, after performing one-way ANOVA tests on the fibrillar apparent modulus population mean among the entire uncycled (C, O, A, B), 5-cycle (A, B), and 10-cycle sample populations (B), no statistically significant difference was found. There was also no significant difference between mean fibrillar apparent moduli measured at each treatment level for any single individual sample.

Average residual strains, strains present in the sample without the application of an outside stress, were measured at each point for all of the samples at each freezing treatment. The average residual HAP strains were −1500 ± 330 με, −1500 ± 270 με, and −1500 ± 320 με for the uncycled samples (A, B, C, O), the samples frozen 5 times (A, B) and those frozen 10 times (A), respectively. The values are not significantly different from each other as shown in Fig. 7. For samples that were uncycled, cycled 5 times, and cycled 10 times, the average fibrillar residual strains were 0 με, −170 ± 40 με, and −400 ± 610 με. Since there is no option to achieve an absolute measurement of the residual strain in the collagen fibrils, these measurements are relative to the strain measured in the samples at zero load before any treatment, which was defined to be zero. The residual strain measured after 5 and 10 freezing cycles was then compared to those measured in the uncycled samples to obtain the variation in residual strains with treatment. The average residual strains measured after the first and
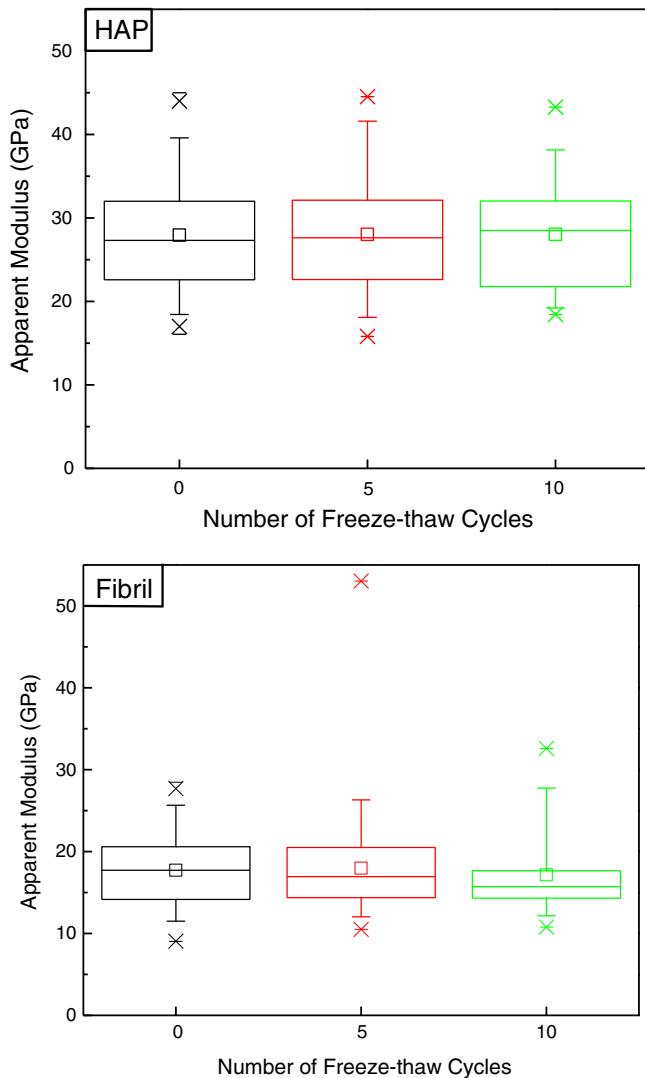
Fig. 6. Box plots showing the mean (□), maximum and minimum values (−), as well as the 99th and 1st (x), 95th and 5th (whiskers), and 75th, 50th, and 25th percentiles (box) for HAP and the fibril apparent modulus for the entire populations of samples uncycled (12 specimens: O, A, B, C), after 5 freeze–thaw cycles (6 specimens: A, B), and after 10 freeze–thaw cycles (3 specimens: A).
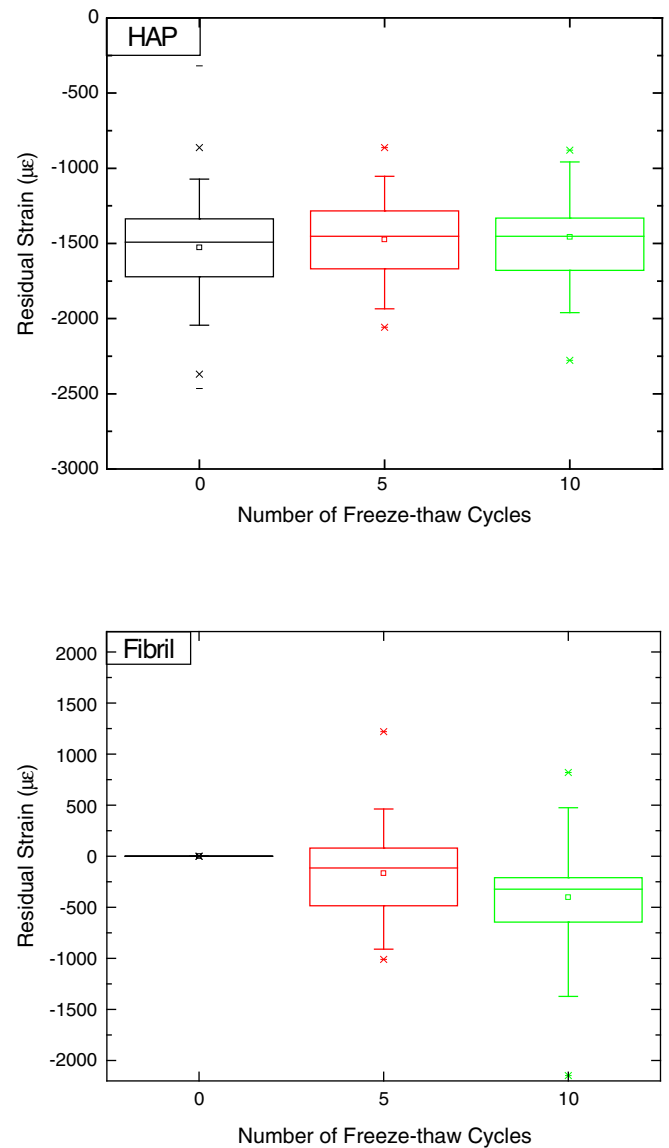
Fig. 7. Box plots showing the mean (□), maximum and minimum values (−), as well as the 99th and 1st (x), 95th and 5th (whiskers), and 75th, 50th, and 25th percentiles (box) for HAP and fibril residual strain for the entire populations of samples uncycled (12 specimens: O, A, B, C), after 5 freeze–thaw cycles (6 specimens: A, B), and after 10 freeze–thaw cycles (3 specimens: A).

second rounds of freezing are not significantly different from each other but are both significantly different from zero strain.

4. Discussion

The lack of change in the apparent elastic moduli of HAP or the fibril in the dentin as a function of freeze–thaw cycling strongly suggests that such cycling has little to no effect on the load transfer behavior between collagen and HAP in dentin, at least up to 10 cycles. Although this study was performed with a narrow range of samples, these are not three random populations but rather three populations initially similar and related to each other by the number of freeze–thaw cycles. Therefore, if freezing was having a measurable effect on the elastic properties of the dentin, such as significant degradation of dentin, a trend would be expected with increasing cycle number, i.e. an increase in the HAP apparent modulus indicating reduction in load transfer capability due to damage. However, no change in the average value of the HAP apparent modulus was detected. Similarly, if freezing damage was denaturing the collagen, a decrease in the average fibrillar apparent modulus would be expected, and yet only a small decrease is measured after 10 freeze–thaw cycles. This strongly suggests that HAP and fibrillar apparent elastic moduli, and therefore the load transfer behavior of the two phases in dentin, do not change significantly after 5 or 10 freeze–thaw cycles.

Damage by cracking from volume expansion of water in the tubules, as suggested by Ref. [8] for human adult dentin, would cause unloading near the crack faces and stress concentration near the crack tip, therefore causing a change in average apparent phase moduli due to local changes in stress and therefore strains of the two constituent phases. However, the nature of the experimental setup in this study makes it difficult to measure the effects of such cracks due to crack closure during thawing and compressive loading. Furthermore, since each of the diffraction strain measurements is averaged over an approximate volume of 6×10^{-3} mm^3, localized damage (such as cracks) at a scale well below this volume may not be detected. Examination of the trends in the residual strains of the samples at each level of treatment can provide some information. If cracks were forming around many of the tubules and propagating through the dentin sample, a significant portion of the initial residual strain present in the sample would be released. The results show, however, no measurable change in the HAP residual strain before or after freeze–thaw cycling up to 10 cycles. Even more surprising is the fact that the fibrillar residual strain becomes more compressive after freeze–thaw cycling, suggesting that during cracking the HAP platelets are coming closer together. More likely, the platelets' spacing is decreasing due to collagen sliding caused by the loading of the samples during measurements. The lack of decrease in the residual strains suggests that high levels of cracking due to water expansion in the tubules do not occur under these experimental conditions.

The average values for the HAP apparent moduli in the samples that were cycled 0, 5, and 10 times are all higher than the value of 18 GPa, as previously reported for similar measurements on a single deciduous bovine incisor dentin sample from a different cow subjected to about 3 freeze–thaw cycles [15]. This value however is within the range of apparent moduli measured here. This is evidence for the great variability of elastic properties between samples. Similarly, the variation in the average standard deviations between treatments is attributed to differences in the number of samples in each population. With the population decreasing from twelve for the uncycled population, to six for the 5-cycle population and finally to three for the 10-cycle population, the effect of individual samples increases with the decrease in population size. Also, although great care was taken to sample with X-rays in the same locations in each dentin cylinder after freezing treatments, slight variations in position are possible. This change in location from one measurement to another on a given sample, on the order of 100 μm or about three times the beam size, may affect the measured apparent modulus because of strain heterogeneities.

5. Conclusions

The present synchrotron X-ray diffraction study measured, in bovine dentin, the load transfer between the HAP crystals and the collagen matrix, which is a sensitive measure of damage in the materials. As compared to uncycled samples, samples subjected to five, and ten freeze–thaw cycles show no statistically significant change in the level of load transfer. Therefore, bovine dentin may be safely stored in frozen PBS at −25 °C and subjected to multiple freeze–thaw cycles with no significant effect to the load transfer properties as measured by high-energy synchrotron X-ray diffraction.

References

[1] I.A.M. de Graaf, H.J. Koster, Toxicol. Vitro 17 (2003) 1–17.
[2] M. Salai, T. Brosh, N. Keller, M. Perelman, I. Dudkiewitz, Cell Tissue Bank. 1 (2000) 69–73.
[3] J. Camps, P. Martin, P. Ladeque, R. Rieu, J. Fuseri, Dent. Mater. 10 (1994) 210–214.
[4] J. Camps, X. Baudry, V. Bordes, J. Dejou, C. Pignoly, P. Ladeque, Dent. Mater. 12 (1996) 121–126.
[5] H. Moscovich, N.H.J. Creugers, J.A. Jansen, J.G.C. Wolke, J. Dent. 27 (1999) 503–507.
[6] E.D. Sedlin, Acta Orthop. Scand. Suppl. 83 (1965) 20–21.
[7] K.-I. Tonami, H. Takahashi, F. Nishimura, Dent. Mater. J. 15 (1996) 205–211.
[8] G. Guidoni, J. Denkmayr, T. Schoberl, I. Jager, Philos. Mag. 86 (2006) 5705–5714.
[9] D.K. Moon, S.L.-Y. Woo, Y. Takakura, M.T. Gabriel, S.D. Abramowitch, J. Biomech. 39 (2006) 1153–1157.
[10] S. Giannini, R. Buda, F. Di Caprio, P. Agati, A. Bigi, V. De Pasquale, A. Ruggeri, Int. Orthop. 32 (2008) 145–151.
[11] C.W. Smith, I.S. Young, J.N. Kearney, J. Biomech. Eng. 118 (1996) 56–61.
[12] P. Clavert, J.-F. Kempf, F. Bonnomet, P. Boutemy, L. Marcelin, J.L. Kahn, Surg. Radiol. Anat. 23 (2001) 259–262.
[13] J.D. Almer, S.R. Stock, J. Struct. Biol. 152 (2005) 14–27.
[14] J.D. Almer, S.R. Stock, J. Struct. Biol. 157 (2007) 365–370.
[15] A.C. Deymier-Black, J.D. Almer, S.R. Stock, D.R. Haeffner, D.C. Dunand, Acta Biomater. 6 (2010) 2172–2180.
[16] R. Akhtar, M.R. Daymond, J.D. Almer, P.M. Mummery, J. Mater. Res. 23 (2008) 543–550.
[17] H.S. Gupta, J. Seto, W. Wagermaier, P. Zaslansky, P. Boesecke, P. Fratzl, PNAS 103 (2006) 17741–17746.
[18] H.S. Gupta, W. Wagermaier, G.A. Zickler, J. Hartmann, S.S. Funari, P. Roschger, H.D. Wagner, P. Fratzl, Int. J. Fract. 139 (2006) 425–436.
[19] H.S. Gupta, W. Wagermaier, G.A. Zickler, D. Raz-Ben Aroush, S.S. Funari, P. Roschger, H.D. Wagner, P. Fratzl, Nano Lett. 5 (2005) 2108–2111.
[20] R.G. Craig, F.A. Peyton, J. Dent. Res. 37 (1958) 710–719.
[21] M.R. Daymond, M.L. Young, J.D. Almer, D.C. Dunand, Acta Mater. 55 (2007) 3929–3942.
[22] M.L. Young, J.D. Almer, M.R. Daymond, D.R. Haeffner, D.C. Dunand, Acta Mater. 55 (2007) 1999–2011.
[23] A. Wanner, D.C. Dunand, Metall. Mater. Trans. A-Phys. Metall. Mater. Sci. 31 (2000) 2949–2962.
[24] M.L. Young, J.D. DeFouw, J.D. Almer, D.C. Dunand, Acta Mater. 55 (2007) 3467–3478.
[25] M.L. Young, J.D. Almer, U. Lienert, D.R. Haeffner, R. Rao, J.A. Lewis, D.C. Dunand, Affordable Metal Matrix Composites for High-Performance Applications II, 2003, pp. 225–233.
[26] B.B. He, K.L. Smith, SEM Spring Conference on Experimental and Applied Mechanics and Experimental/Numerical Mechanics in Electronic Packaging III, Houston, TX, 1998.
[27] O. Cornu, X. Banse, P.L. Docquier, S. Luyckx, C. Delloye, J. Orthop. Res. 18 (2000) 426–431.
[28] J.D. Currey, J. Foreman, I. Laketic, J. Mitchell, D.E. Pegg, G.C. Reilly, J. Orthop. Res. 15 (1997) 111–117.